

UDK 691.73; 622.785

## **Densification and Volumetric Change During Supersolidus Liquid Phase Sintering of Prealloyed Brass Cu<sub>28</sub>Zn Powder: Modeling and Optimization**

**A. Mohammadzadeh<sup>1,\*</sup>, M. Azadbeh<sup>2</sup>, A. Sabahi Namini<sup>2</sup>**<sup>1</sup>Young Researchers and Elite Club, Ahar Branch, Islamic Azad University, Ahar, Iran<sup>2</sup>Department of Materials Engineering, Sahand University of Technology, P.O. Box 51335-1996, Tabriz, Iran

---

**Abstract:**

*An investigation has been made to use response surface methodology and central composite rotatable design for modeling and optimizing the effect of sintering variables on densification of prealloyed Cu<sub>28</sub>Zn brass powder during supersolidus liquid phase sintering. The mathematical equations were derived to predict sintered density, densification parameter, porosity percentage and volumetric change of samples using second order regression analysis. As well as the adequacy of models was evaluated by analysis of variance technique at 95% confidence level. Finally, the influence and interaction of sintering variables, on achieving any desired properties was demonstrated graphically in contour and three dimensional plots. In order to better analyze the samples, microstructure evaluation was carried out. It was concluded that response surface methodology based on central composite rotatable design, is an economical way to obtain arbitrary information with performing the fewest number of experiments in a short period of time.*

**Key words:** Brass alloy, Supersolidus liquid phase sintering, Response surface methodology.

---

### **1. Introduction**

Brass powders are commonly produced from atomization technology with a composition of 10, 20, and 30 wt. % of Zn in part with further alloying elements. Sintering of brass prealloyed powder is normally performed at temperature range from 815 to 925 °C depending on alloy composition [1, 2]. This feature is useful in performing supersolidus liquid phase sintering (SLPS), where liquid forms when heated just over the solidus temperature.

The commonly observed liquid formation sites are the grain boundaries within a particle, the interparticle neck region and the grain interior. Liquid forms inside the particles and spreads to the particle contacts, resulting in capillary force acting on the semisolid particles and enhances the densification [3-10]. Densification of brass during sintering by SLPS is sensitive to time and temperature. Increasing sintering time leads to grain coarsening that can be illustrated with equation (1) as followed:

$$G^n - G_0^n = Kt \quad (1)$$

where K is the grain growth rate constant, n is constant, and G<sub>0</sub> is the initial grain size [3, 10].

---

\*) **Corresponding author:** amzadeh@ymail.com

To avoid distortion or blistering of the compacts, sintering temperatures should not exceed the critical temperature of the alloy [9, 11]. A limitation of SLPS is that the condition necessary for densification are often very close to the condition resulting in compact shape distortion and microstructural changes due to interplay of capillary and gravity force, so that a high liquid formation results in rapid densification, but less dimensional precision [12-16].

To optimize sintering process, one of the important things to know is the relationship between the variables of interest, which is the optimization object (e.g., the sintered density which used to evaluate densification) and the system factors, which are the sintering variables. A large number of experimental investigations have been carried out which only few of them substantiated their observations with a theoretical model. However, present day industrial application demands comprehensive theoretical simulation before actual design [17].

Response surface methodology (RSM) is a collection of mathematical and statistical techniques that is useful for the modeling, analyzing, and optimizing of an object in which a response of interest is influenced by several parameters [18]. RSM also quantifies the relationship between the controllable input parameters and the obtained responses. The steps in this method involve:

- Designing a series of experiments for adequate and reliable measurement of the response of interest;
- Determining a mathematical model of the second-order response surface with the best fit;
- Finding the optimal set of experimental parameters that produce a maximum or minimum value of response; and
- Representing the direct and interactive effects of process parameters through two and three dimensional plots [18-20].

In recent years numerous researchers have been used design of experiments (DOE) to analyze and model the powder metallurgy technique key parameters. C. H. Ji et al. [21] investigated the effect of sintering parameters such as sintering temperature, sintering time, heating rate, and sintering atmosphere on the sintered density using Taguchi method, based on orthogonal arrays (OA), which is widely used in research and industrial application. P. K. Bardhan et al. [17] established empirical relationships to predict sintered density of ferrous powder using second order RSM based on central composite design (CCD). In another work P. K. Bardhan et al. [22] has used CCD method to analyze the surface roughness value of sintered iron powder metallurgy components. M. Joseph Davison et al. [23] works focused on the two of the techniques namely Neural Network (NN) and RSM for predicting the final density of sintered aluminum performs.

In this study RSM based on central composite rotatable design (CCRD) has been used to establish the functional relationships between two SLPS variables namely sintering temperature and time, for evaluating and modeling responses (sintered density, densification parameter, porosity percentage and volumetric changes). These relationships can provide mathematical models based on empirical results that can be used to analyze and predict the responses and to determine the optimal SLPS variables. The analysis of variance (ANOVA) shows that experimental results fit well into the assumed CCRD models.

## **2. Experimental procedure**

### **2.1. Manufacturing of specimens**

Water atomized prealloyed brass powder provided by Tabriz Powder Metallurgy Company was used as the base material. The characteristics and properties of powder have been determined by sieving method (ASTM E11 standard), flowability (ASTM B213 standard), apparent density (ASTM B212 standard), and X-ray fluorescence (XRF) analysis

for chemical composition. In order to determine sintering temperature range differential scanning calorimetry (DSC) was carried out from brass prealloyed powder in a heating rate of 20 °C/min. The powder was mixed with 0.75 wt. % lithium stearate as lubricant in a V shaped mixer at 65 rpm for a period of 60 min. The mixed powders, used as the base material of all compacts, were briquetted in to rectangular bars of 55mm×10mm×10mm using a pressure of 600 MPa in a uniaxial hydraulic press. The green density was calculated by measuring the compacts weight and dimensions. The heating cycle included a 30 min dwell at 540 °C for de lubricating followed by sintering at different temperatures and times in a small laboratory furnace (type, TFS/25-1250) with three heating zones, as shown schematically in Fig. 1. A flowing of N<sub>2</sub> industrial gas, equal to 2 l/min, was maintained throughout the entire cycle. After sintering, the boat was pushed into the water-jacketed exit zone.

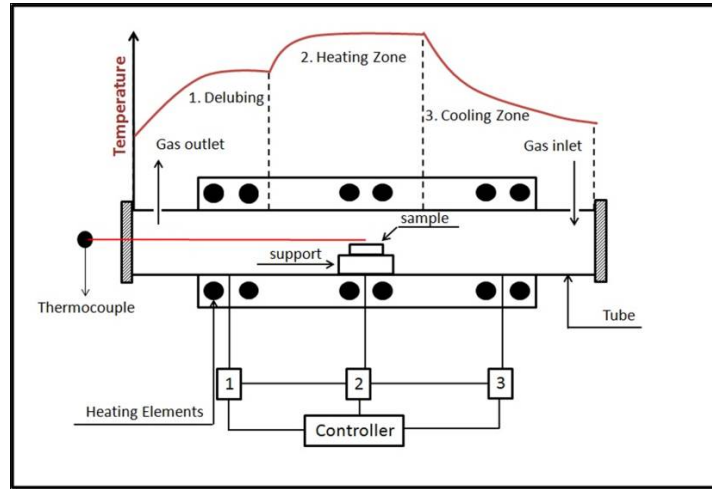


**Fig. 1.** Schematic sketch of tube furnace and temperature controlling process.

The sintered specimens were characterized by measuring density through water displacement by Archimedes method (DIN ISO 3369) according to equation (2), since this technique is more precise than calculating the density from the dimensions as done with the green compacts.

$$\rho_s = \frac{M_1}{M_2 - M_3} \times \rho_w \quad (2)$$

Here  $\rho_s$  is sintered density (g/cm<sup>3</sup>),  $M_1$ = weight in air (g),  $M_2$ = weight of water proofed sample (g),  $M_3$ = weight in water (g) and  $\rho_w$ = water density (g/cm<sup>3</sup>). The degree of densification after sintering was measured using a densification parameter,  $\psi$ , which is expressed as:

$$\psi = \frac{\rho_s - \rho_g}{\rho_t - \rho_g} \times 100 \quad (3)$$

where,  $\psi$  is densification parameter,  $\rho_g$  is green density (g/cm<sup>3</sup>), and  $\rho_t$  is theoretical density (g/cm<sup>3</sup>) which was calculated using the inverse rule of mixtures through the following formula:

$$\frac{1}{\rho_t} = \sum_i \frac{w_i}{\rho_i} \quad (4)$$

where N is the number of elements in the mixture,  $w_i$  is the weight fraction of i<sup>th</sup> component, and  $\rho_i$  is the theoretical density of i<sup>th</sup> element [24].

Furthermore, porosity percentage was calculated using equation (5) [25]:

$$\%Porosity = (1 - \frac{\rho_s}{\rho_t}) \times 100 \quad (5)$$

As well as the volumetric change or shrinkage was measured from equation (6):

$$\%Volumetric\ Change = \frac{V_s - V_g}{V_g} \quad (6)$$

where  $V_g$  is the green samples volume which calculated by measuring dimensions of specimens and  $V_s$  is the sintered samples volume which determined by Archimedes method ( $V_s = M_2 - M_3$ ).

The sintered specimens were sectioned in parallel to the pressing direction, polished and etched (8 g FeCl<sub>3</sub>, 25 ml HCl, 50 ml H<sub>2</sub>O). Microstructural examination of the etched specimens was conducted using an optical microscopy.

## 2.2. Response Surface Methodology (RSM)

Design of experiments is an empirical and analytical technique for setting efficient process parameters which has significant effect on the response of interest. Full factorial design, fractional factorial design, and central composite rotatable design (CCRD) are the most applicable methods in design of experiments. CCRD is a method for design of experiments which was originally developed by Box and Wilson (1951) [20, 26]. Hence, in this study CCRD, consists of 13 sets of runs; two selected independent SLPS variables (temperature and time), was used for design of experiments. The value of SLPS variables and their levels involved in this research are listed in Tab. I.

**Tab. I** Symbols, levels and values of SLPS variables.

Symbols	SLPS variables	Units	Type	Subtype	Coded values of variables				
					-1.41	-1	0	1	1.41
A	Temperature	°C	Numeric	Continuous	840	850	875	900	910
B	Time	min	Numeric	Continuous	6	15	38	60	70

**Tab. II** Design layout using the Design-Expert 8.0 software including experimental and predicted results for sintered density, densification parameter and porosity percentage.

Standard order	Runs	Coded values		Sintered density [g.cm <sup>-3</sup> ]		Densification parameter [%]		Porosity [%]	
		A	B	Actual value	Predicted value	Actual value	Predicted value	Actual value	Predicted value
1	3	-1	-1	6.87	6.76	12.35	5.51	17.13	18.42
2	5	1	-1	7.3	7.18	36.54	29.48	11.94	13.37
3	2	-1	1	7.18	7.21	32.32	34.23	13.39	12.98
4	7	1	1	7.29	7.31	39.02	40.7	12.06	11.8
5	8	-1.41	0	6.79	6.83	8.54	11.01	18.09	17.67
6	6	1.41	0	7.13	7.18	29.27	32.06	13.99	13.37
7	9	0	-1.41	6.9	7.05	11.47	20.44	16.77	15.02
8	10	0	1.41	7.5	7.45	51.53	48.04	9.53	10.19
9	4	0	0	7.42	7.43	46.63	47.06	10.5	10.34
10	13	0	0	7.43	7.43	47.56	47.06	10.37	10.34
11	12	0	0	7.43	7.43	45.22	47.06	10.37	10.34
12	11	0	0	7.43	7.43	47.23	47.06	10.37	10.34
13	1	0	0	7.46	7.43	49.08	47.06	10.01	10.34

The measured responses were the sintered density, densification parameter, porosity percentage, and volumetric change percentage. The results obtained through the experiments, which were done randomly, and predicted values for responses are summarized in Tab. II and III. The available data and design of experiments have been analyzed by using Design-Expert 8.0 software [27].

**Tab. III** Design layout using the Design-Expert 8.0 software including experimental and predicted results for volumetric change.

Standard order	Runs	Coded values		Volumetric change [%]	
		A	B	Actual value	Predicted value
1	3	-1	-1	-6.21	-4.61
2	5	1	-1	-10.24	-8.63
3	2	-1	1	-12.19	-12.59
4	7	1	1	-11.81	-12.2
5	8	-1.41	0	-7.02	-7.63
6	6	1.41	0	-9.47	-10.1
7	9	0	-1.41	-4.24	-6.31
8	10	0	1.41	-15.13	-14.35
9	4	0	0	-12.78	-13.2
10	13	0	0	-13.51	-13.2
11	12	0	0	-12.78	-13.2
12	11	0	0	-13.51	-13.2
13	1	0	0	-13.51	-13.2

### 2.3. Development of mathematical models

In this research, the SLPS variables were mathematically related to the empirically obtained response functions (sintered density, densification parameter, porosity percentage, and volumetric change percentage). A second order polynomial regression model has been developed for evaluation of effects of all variables. The responses are a function of sintering temperature (A, °C) and sintering time (B, min) that can be expressed as follows:

$$Y = f(A, B) \quad (7)$$

where, Y is a response value. The second order regression equation which is used in this research to represent the response surface for k factors is given by (8):

$$Y = a_0 + \sum_{i=1}^k a_i X_i + \sum_{i=1}^k a_{ii} X_i^2 + \sum_{i < j} a_{ij} X_i X_j \quad (8)$$

where,  $X_i$  and  $X_j$  are the coded independent variables,  $a_0$  is the free term of equation and  $a_i$ ,  $a_{ii}$  and  $a_{ij}$  are linear, quadratic, and interaction constant coefficients, respectively [7, 14]. The selected polynomial could be expressed as (9):

$$Y = a_0 + a_1 A + a_2 B + a_{12} AB + a_{11} A^2 + a_{22} B^2 \quad (9)$$

where the letters A and B represent the factors in the model and their combinations (such as AB) represent an interaction between the individual factors in that term.

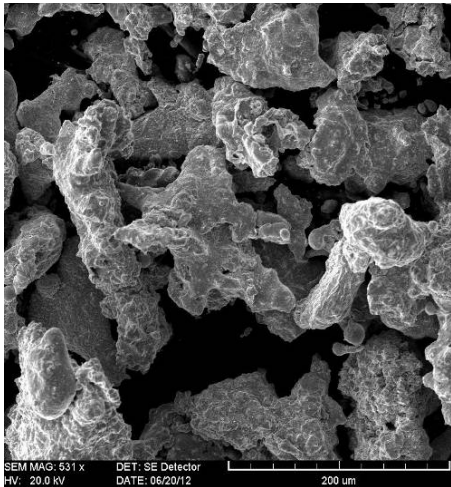
The coefficients values of equation (9) were calculated by regression method using Design-Expert 8.0 software at 95% confidence level. The regression coefficients of second order polynomial regression model were calculated by experimental data shown in Tab. II, III. Also, in order to ensure model accuracy, ANOVA analysis was performed.

### 3. Results and discussion

#### 3.1. Material characteristics

The characteristics and chemical analysis of starting brass powder are given in Tab. IV.

**Tab. IV** Morphology and characteristics of the used brass powder.

Powder morphology	Chemical analysis	
	Cu	Balance
	Zn	28.6
	Al	0.14
	Fe	0.085
	S	0.062
	Si	0.054
	P	0.0084
<b>Brass powder properties</b>		
Flowability [sec/50g]	21	
Apparent density [g/cm <sup>3</sup> ]	3.2	
Powder shape	Irregular	
<b>Sieve analysis results</b>		
9.75 wt. %	125-180 μm	
24.63 wt. %	90-125 μm	
23.53 wt. %	63-90 μm	
39.77 wt. %	<63 μm	

Also calculated theoretical density according to equation (4), using the results of chemical analysis, was equal to 8.29 g/cm<sup>3</sup>. As well as green density of samples was measured equal to 6.65±0.01 g/cm<sup>3</sup>.

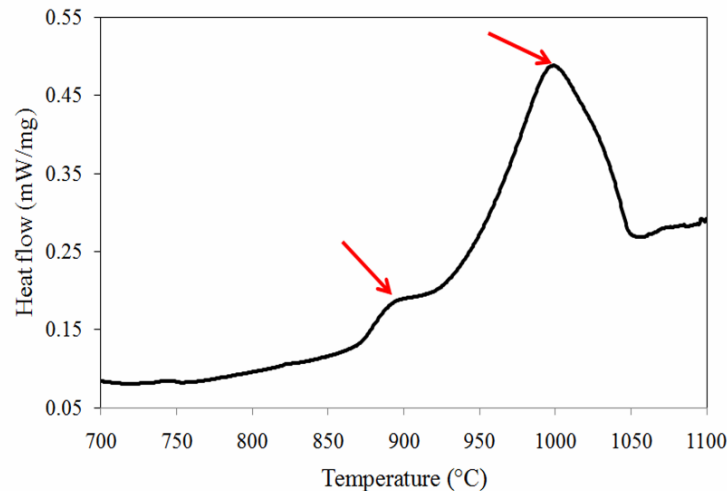


**Fig. 2.** DSC curve of Cu28Zn brass prealloyed powder.

Sintering temperature range was determined using DSC curve obtained on used powder (Fig. 2). There are some peaks on the heating step in temperature range of 700 °C to 1200 °C which show two endothermic peaks. By comparing the peaks intensity the first

endothermic peak is indubitably referred to the brass melting since Cu-Zn alloy of given chemical composition melts between 850 °C and 900 °C. The second endothermic peak according to its higher intensity can stand for the transformation of liquid to vapor which due to boiling point of zinc can be concluded that zinc evaporation has occurred. Therefore, temperature window of 850 °C to 900 °C is suitable for designing experiments.

### 3.2. Development of mathematical models

Second order polynomial regression models proposed by Design Expert-8 software are given in equations (10) to (13) for response variables.

$$\text{Sintered density [g.cm}^{-3}] = 7.43 + 0.13A + 0.14B - 0.08AB - 0.22A^2 - 0.093B^2 \quad (10)$$

$$\text{Densification parameter [\%]} = 46.84 + 7.61A + 9.99B - 4.37AB - 13.02A^2 - 6.34B^2 \quad (11)$$

$$\text{Porosity [\%]} = 10.38 - 1.56A - 1.75B + 0.97AB + 2.64A^2 + 1.12B^2 \quad (12)$$

$$\text{Volumetric change [\%]} = -13.13 - 0.91A - 2.89B + 1.1AB + 2.21A^2 + 1.42B^2 \quad (13)$$

The presented models are based on coded values of variables. The symbols A and B show sintering temperature and time, respectively.

### 3.3. Checking adequacy of the models

Adequacy of the models was tested using analysis of variance (ANOVA), normality and regression analysis. Tab. V presents ANOVA for response variables by higher precision at 95% confidence level.

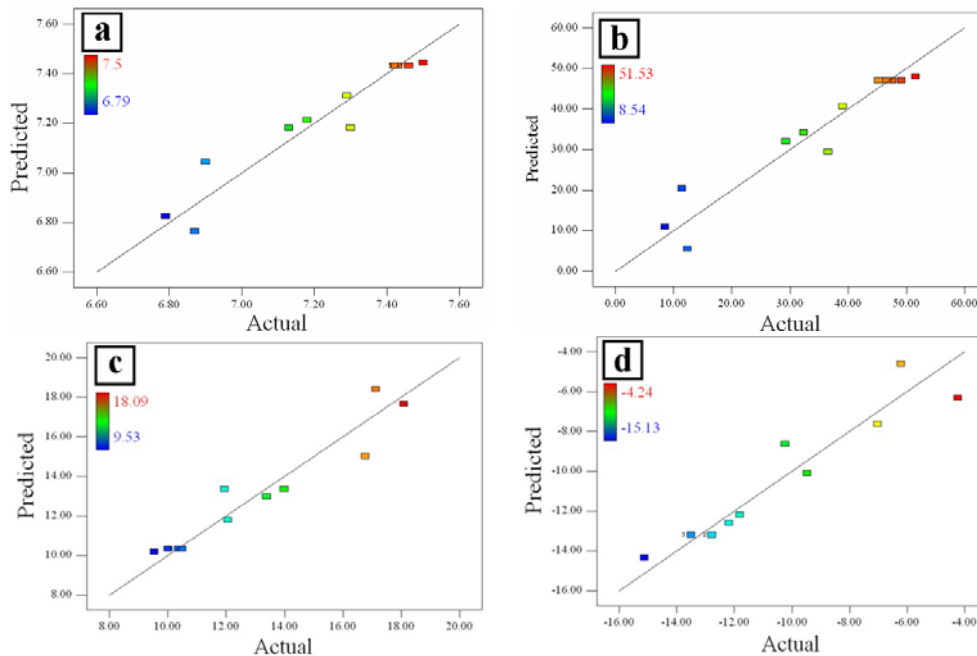


**Fig. 3.** Plot of predicted response vs. actual value for; (a) sintered density [g/cm<sup>3</sup>], (b) densification parameter [%], (c) porosity [%], (d) volumetric change [%].

According to F-values and R<sup>2</sup> it can be concluded that equations (10) to (13) have high validity and can be applied to predict the responses. Calculated R<sup>2</sup> and Adj. R<sup>2</sup> values for all responses verify that the predicted and actual response values are in good agreement with

each other (See Fig. 3). The normal probability plots indicate that the points follow approximately a straight line (Fig. 4) and the residuals have a normal distribution, consequently. As well as it is obvious that the errors are spread normally.

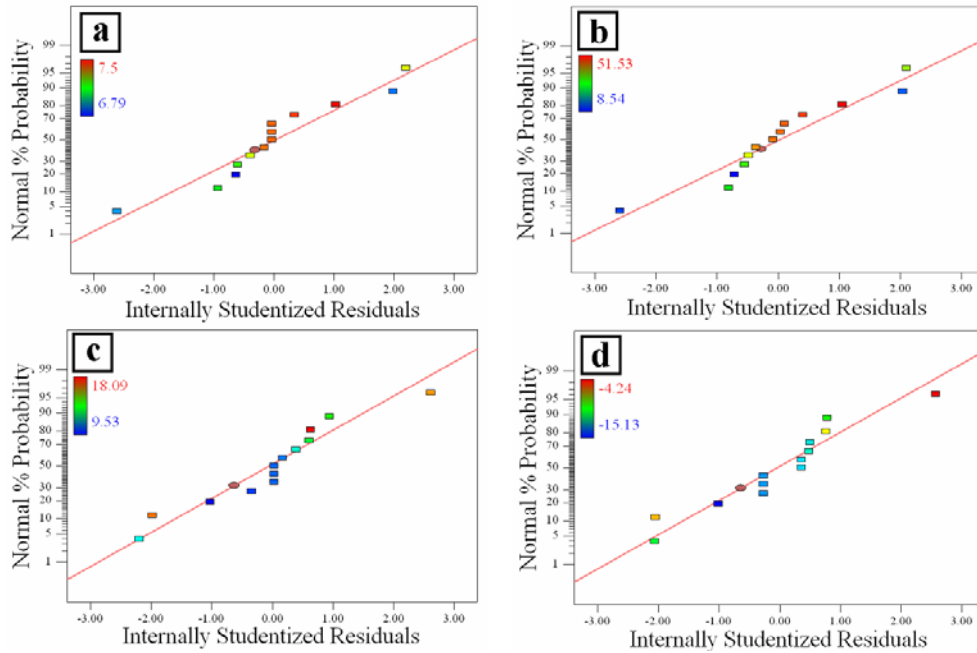


**Fig. 4.** Normal probability plot of residuals for responses; (a) sintered density [ $\text{g}/\text{cm}^3$ ], (b) densification parameter [%], (c) porosity [%], (d) volumetric change [%].

**Tab. V** ANOVA table;  $R_1$ : Sintered density [ $\text{g}\cdot\text{cm}^{-3}$ ],  $R_2$ : densification parameter [%],  $R_3$ : porosity [%] and  $R_4$ : volumetric change [%].

Response	Sum of squares		Mean squares		df		F-value	$R^2$	Adj. $R^2$
	Reg.	Residual	Reg.	Residual	Reg.	Residual			
$R_1$	0.68	0.056	0.14	$7.95 \times 10^{-3}$	5	7	17.16	0.9241	0.87
$R_2$	2626.1	217.54	525.22	31.08	5	7	16.9	0.9235	0.8689
$R_3$	98.65	8.1	19.73	1.16	5	7	17.05	0.9241	0.8699
$R_4$	119.95	11.79	23.99	1.68	5	7	14.24	0.9105	0.8465

\* df: Degree of freedom and Reg.: Regression.

### 3.4. Evaluating the effect of temperature and time on SLPS process

To demonstrate the influence of sintering temperature and time on responses, perturbation plots have been used.

In Fig. 5a and 5b the influence of temperature and time on sintered density and densification parameter is shown. It is seen that when time is assumed constant (equal to 37.5 minutes), diagram follows parabolic behavior and almost around the central point ( $875^\circ\text{C}$ ) maximum value for density is attained (curve A). Assuming temperature is constant at the central point, the effect of time on density can be seen (curve B). The influence of sintering time on densification is almost similar to sintering temperature effect.

Fig. 5c and 5d show porosity percentage and volumetric change variation with sintering temperature and time. It can be concluded that around the central point the lowest



porosity and the highest volumetric change obtained and this result corresponds well with the maximum density and densification parameter at this area.

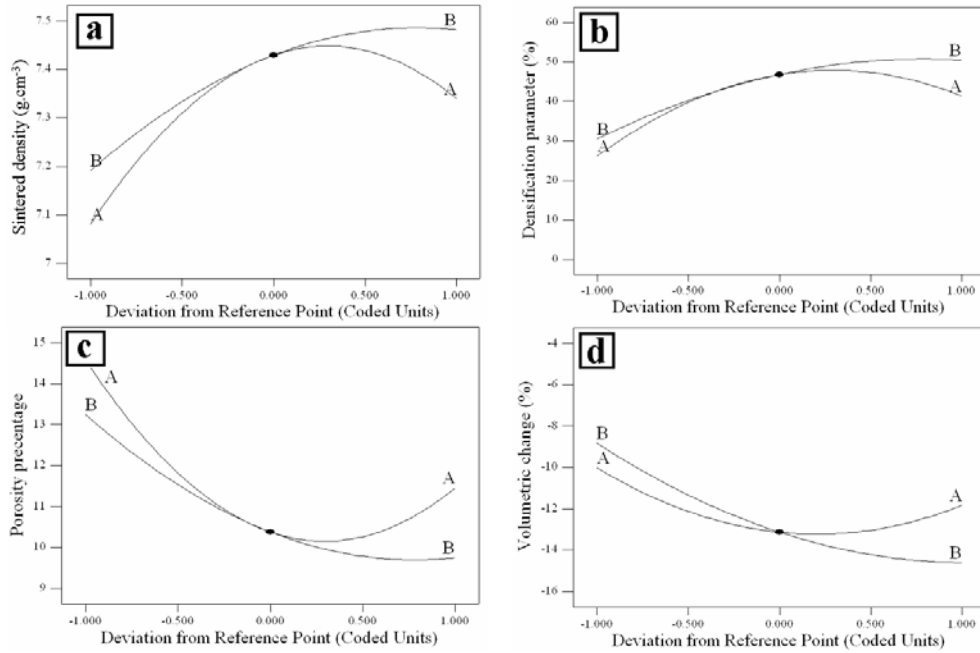


**Fig. 5.** Perturbation plots for responses at the central points of the design space (a) sintered density [g/cm<sup>3</sup>], (b) densification parameter [%], (c) porosity [%], (d) volumetric change [%].

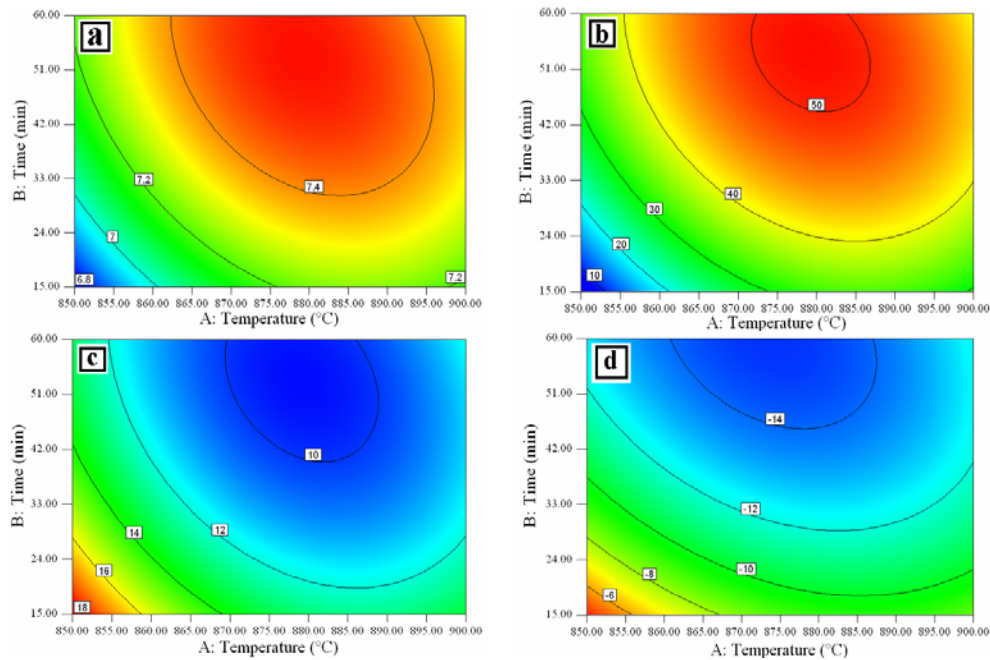


**Fig. 6.** Contour plots of responses; (a) sintered density [g/cm<sup>3</sup>], (b) densification parameter [%], (c) porosity [%], and (d) volumetric change [%].

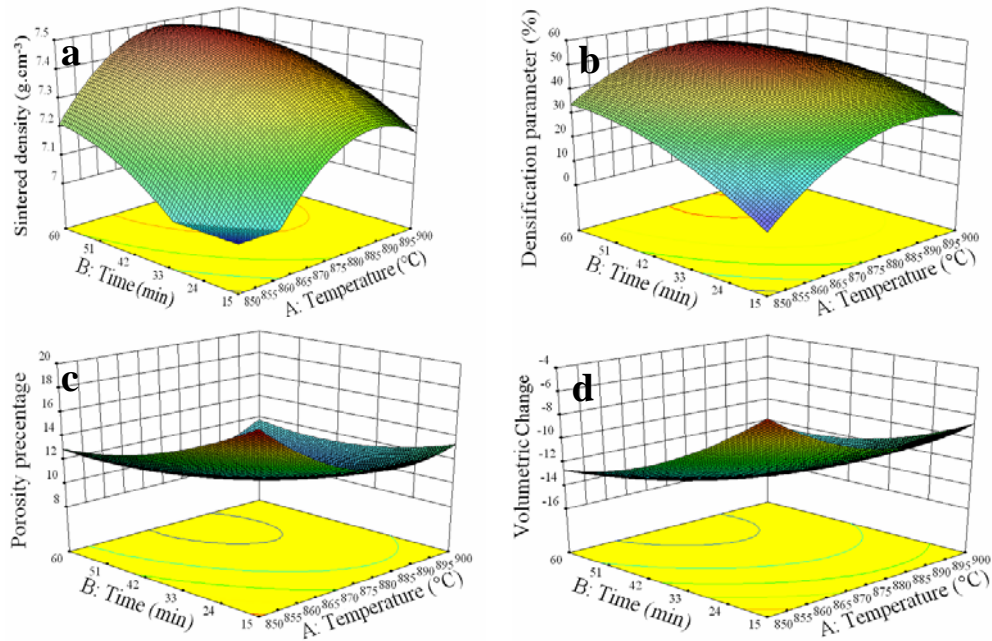


**Fig. 7.** Three dimensional plots of responses; (a) sintered density [ $\text{g}/\text{cm}^3$ ], (b) densification parameter [%], (c) porosity [%], (d) volumetric change [%].

According to Figs. 6 and 7 the interaction of sintering temperature and time on responses were investigated, using contour plots and three dimensional surfaces. It is shown that the maximum amount of density and densification parameter, and the minimum amount of porosity percentage and the maximum amount of volumetric change (shrinkage) are achieved at a point proximity of the central point (875 °C, 37.5 min). Three dimensional plots (Fig. 7) confirm parabolic behavior of density, densification parameter, porosity percentage and volumetric change against time and temperature. Hence, it is recommended to use the red area of contour plots to achieve maximum sintered density and densification parameter (Fig. 6a and 6b).

### 3.5. Optimization of SLPS process

In Tab. VI, the conditions for getting each desired responses are summarized. So if densification has significant importance, suggested sintering temperature and time are 880 °C and 54 min, respectively.

**Tab. VI** Optimum conditions for responses; R<sub>1</sub>: Sintered density [ $\text{g}/\text{cm}^3$ ], R<sub>2</sub>: densification parameter [%], R<sub>3</sub>: porosity [%] and R<sub>4</sub>: volumetric change [%].

Response	Goal	Sintering temperature (°C)	Sintering time (min)	Predicted	Desirability
R <sub>1</sub>	Max	879	54	7.49	0.988
R <sub>2</sub>	Max	879	54	51.13	0.991
R <sub>3</sub>	Min	879	53	9.63	0.988
R <sub>4</sub>	Min	874	60	-14.61	0.952

It seems that, in order to achieve the maximum amount of volumetric change (shrinkage), the proposed temperature and time are proximity the same for maximum densification. Thus in

manufacturing of brass components made from prealloyed powder the amount of dimensional changes during sintering should be considered.

### 3.6. Microstructural evaluation

To give a good reference to the process taking place after an increase in sintering temperature and time, metallography examinations were done. By increasing sintering temperature and time the amount of formed liquid is augmented and rearrangement of grains is developed. When studying the microstructure of the sintered samples (Fig. 8), the main interest was focused on pore elimination. Grain growth and pore enlargement were also observed with increasing sintering temperature and time. Increasing sintering temperature, rearrangement of fragmented grains of powder particles as a result of further liquid phase formation leads to higher densification and sphericity of grains.

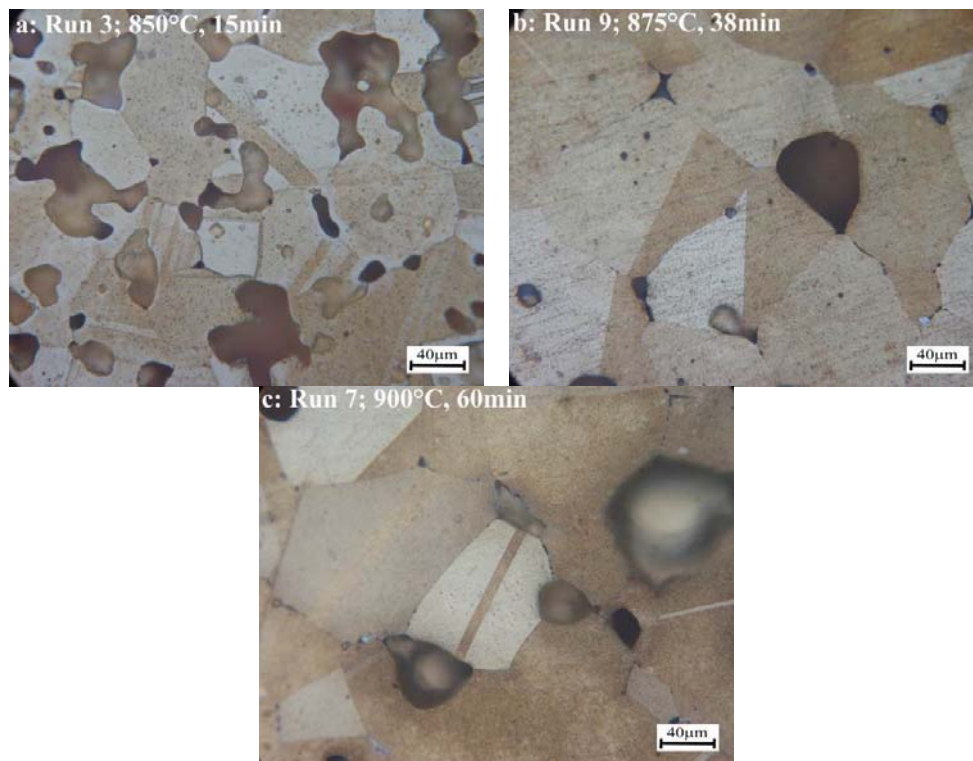


**Fig. 8.** Grain growth and pore enlargement at various sintering temperature and time.

## 4. Conclusion

1. Quadratic mathematical models were developed for modeling sintered density, densification parameter, porosity percentage, and volumetric change percentage at 95% confidence level, and the adequacy of models was analyzed by ANOVA and normal probability plot of residuals. The predictions of proposed models for sintered Cu28Zn brass prealloyed powder in this investigation are in good agreement with the obtained experimental results (at least for the equipment and conditions used here).

2. It is shown that central composite rotatable design (CCRD) is an industrial and economical approach for analyzing and optimizing of SLPS process by performing of fewer experiments.
3. The contour plots and three dimensional surfaces represents that densification and volumetric change have parabolic behavior with sintering temperature and time during SLPS process of prealloyed Cu<sub>28</sub>Zn brass powder.
4. Optimum sintering temperature and time for getting higher densification, determined using Design Expert-8 software, are 880 °C and 54 min. The predicted maximum sintered density and densification parameter were equal to 7.49 g.cm<sup>-3</sup> and 51.13%, respectively.
5. According to microstructural analysis it can be concluded that; low sintering temperature and time due to insufficient interparticle bonding, and high sintering temperature and time because of excess liquid phase formation are not favorable, since, there is an optimum temperature which can contributes to achieving homogenous structure.

## 5. References

1. G. S. Upadhyaya, Sintered metallic and ceramic materials: preparation, properties and applications, Wiley, New York, 1999.
2. A. Sabahi Namini, M. Azadbeh, A. Mohammadzadeh, *Sci Sinter*, 2013, 45, 351-362.
3. R. M. German, *Liquid phase sintering*, Springer, New York, 1985.
4. R. M. German, P. Suri, S. J. Park, *J Mater Sci*, 2009, 44, 1-39.
5. R. M. German, *Int. J. Powder Metall*, 1990, 26, 23-33.
6. R. M. German, *Int. J. Powder Metall*, 1990, 26, 35-43.
7. R. M. German, *Metall Mater Trans A*, 1997, 28, 1553-1567.
8. M. Azadbeh, H. Danninger, C. Gierl-Mayer, *Powder Metall*, 2013, 56, 342-346.
9. Liu, R. Tandon, R.M. German, *Metall Mater Trans A*, 1995, 26, 2423-2430.
10. C. Padmavathi, Anish Upadhyaya, *Sci Sinter*, 2010, 42, 363-382.
11. J. R. Davis, *Copper and copper alloys*, ASM Specialty Handbook, Materials Park OH, 2001.
12. C. S. Marchi, L. Felberbaum, A. Mortensen, *Metall Mater Trans A*, 2000, 31, 397-400.
13. J. Liu, A. Lal, R. M. German, *Acta mater*, 1999, 47, 4615-4626.
14. A. Olevisky, R. M. German, A. Upadhyaya, *Acta mater*, 2000, 48, 1167-1180.
15. Z. S. Nikolic, *Mater Sci Forum*, 2009, 624, 19-42.
16. A. Upadhyaya, R. M. German, *Mater Chem Phys*, 2001, 67, 25-31.
17. P. K. Bardhan, S. Patra, G. Sutradhar, *Materials Sciences and Applications*, 2010, 1, 152-157.
18. A. Heidarzadeh, H. Khodaverdizadeh, A. Mahmoudi, E. Nazari, *Mater Des*, 2012, 37, 166-173.
19. M. Azadbeh, A. Mohammadzadeh, H. Danninger, *Mater Des*, 2014, 55, 633-643.
20. M. Kavanlouei, B. Hashemi, E. Nourafkan, *Journal of Chemical Engineering and Materials Science*, 2011, 2, 53-60.
21. C. H. Ji, N. H. Loh, K. A. Khor, S. B. Tor, *Mater Sci Eng A*, 2000, 311, 74-82.
22. P. K. Bardhan, R. Behera, S. Patra, G. Sutradhar, *International Journal of Scientific & Engineering Research*, 2011, 2, 1-10.
23. M. J. Davidson, N. Selvakumar, A neural network (NN) and response surface methodology (RSM) based prediction model for sintered aluminium performs, *Proceedings of the 11th WSEAS international conference on Artificial Intelligence*,

- 
- Knowledge Engineering and Data Bases; 2012, Cambridge, UK, World Scientific and Engineering Academy and Society (WSEAS), 2012, 48-54.
24. R. Bollina, In situ evaluation of supersolidus liquid phase sintering phenomena of stainless steel 316L: Densification and Distortion, PhD Thesis in Engineering Science and Mechanics, The Pennsylvania State University, 2005.
  25. ASM International Handbook Committee, Heat treating, ASM International, Materials Park OH, 1991.
  26. G. E. P. Box, K. B. Wilson, J Roy Statist Soc, 1951, 13, 1–45.
  27. Cited available at [www.statease.com](http://www.statease.com)

---

**Садржај:** Истражен је метод одзива површине и централно композитно обртни модел ради оптимизације параметара синтеровања на денсификацију  $\text{Cu}_{28}\text{Zn}$  месинганог праха током суперсолидус течног фазног синтеровања. Употребом регресионе анализе другог реда, изведене су математичке једначине којима се предвиђају густине синтеровања, параметри денсификације, проценат порозности и промене у запремини узорака. Исто тако, адекватност модела је процењена варијантном техником и дала 95% поузданости. Коначно, утицај и интеракција варијабли синтеровања ради постизања било ког жељеног својства, приказане су графички у контури и тродимензионално. Ради боље анализе урађена је и микроструктурна евалуација узорака. Закључено је да је метод одговора површине узорка базиран на дизајну централно композитног окрета економични начин прикупљања произвољних информација извођењем малог броја експеримената у кратком временском периоду.

**Кључне речи:** легура месинга, суперсолидус течно фазно синтеровање, метод одзива површине.

---